Polymer Chemistry

Accepted Manuscript

ROYAL SOCIETY OF CHEMISTRY

www.rsc.org/polymers

Journal Name

ARTICLE

Biomacrocyclic Side-Chain Liquid Crystalline Polymers Bearing Cholesterol Mesogens: Facile Synthesis and Topological Effects Study

Received 00th January 20xx,
Accepted 00th January 20xx

DOI: 10.1039/x0xx00000x

www.rsc.org/

Feng Zhou,[a] Yiwen Li,[b] Ganquan Jiang,[a] Zhengbiao Zhang,[a] Yingfeng Tu,[a] Xiaofang Chen,*[a] Nianchen Zhou*[a] and Xiulin Zhu*[a]

Herein we describe the rational design and facile synthesis of biomacrocyclic side-chain liquid crystalline polymers bearing cholesterol mesogens with three different length methylene spacers (m = 2, 6, 11) *via* the combination of reversible addition-fragmentation chain transfer (RAFT) polymerization with Cu(I)-catalyzed azide-alkyne cycloaddition (CuAAC) "click" chemistry. The successful cyclization was confirmed by comprehensive characterization including size-exclusion chromatography (SEC), triple detection size-exclusion chromatography (TD-SEC), Fourier transform infrared (FT-IR) and ^{1}H NMR spectra. Subsequently, the liquid crystalline (LC) phase behaviors of the linear and cyclic polymers were investigated systematically. Both linear and cyclic polymers form smectic phase and exhibit a similar layer periodicity. However, the cyclic ones exhibit a slightly lower mesophase transition temperature, enthalpy, entropy and smaller textures compared with their linear counterparts. Meanwhlie, smectic C (SmC) phase is preferable in cyclic polymer with long methylene spacer (m = 11) compared with that in the linear one.

Introduction

Cyclic polymers have demonstrated unique physical properties in both of solution and solid state compared with their linear analogues due to their "endless" topology.[1] For example, cyclic polymers usually exhibit higher cloud point (T_c),[2a] increased glass transition temperature (T_g),[2b] enhanced fluorescence-emission,[2c] reduced domain spacing[2d] and so on.[2e-2h] Some cyclic polymers have also imparted unique and improved biological properties, such as longer circulation times and improved drug loading and releasing capacity as drug carriers,[3a,3b] as well as reduced cytotoxicity and higher transfection efficiency as gene delivery agents.[3c,3d] In the recent years, the constant demand for new soft materials with sophisticated architectures and improved properties inspires us to develop new strategies for various functional macrocycles.[4]

Liquid crystalline polymers (LCPs) have been extensively studied for several decades due to their wide applications.[5] With the fast growth of this research, rational design and facile synthesis of new LCPs with the non-linear shaped macromolecular architecture became progressively important as new model compounds with diverse distinct and promising proprieties.[6] Among them, the class of cyclic LCPs with LC moieties at different ring locations is particular interesting. For example, Percec et al. reported the polymers bearing main chain macrocycle LC oligomers at the side chain or in main chain.[7a] Subsequently, they precisely synthesized a novel cyclic main-chain LCPs with an odd-even effect.[7b] These cyclic LCPs demonstrated that the macrocyclic conformation induced a profound impact on LC behavior of the polymers. Wan et al. directly connected nonmesogenic cyclic alkylidene terephthalate onto the flexible polyethylene main chain at every repeat unit, resulting in the formation of thermotropic liquid crystalline mesophase due to the steric interaction between flexible main chain and cyclic pendants.[8] Additionally, the side chain liquid crystalline polymers (SCLCPs) have also attracted considerable attentions since the architectures of the polymer can be well designed and more easily constructed by the introduction of wide range of LC mesogens at the polymeric side chain. In 2010, benefiting from the emergence of "intrachain" "click" cyclization methodology, Zhao and co-workers synthesized the first generation of azobenzene-containing cyclic SCLCPs.[9a] It was observed that the topological constraint imposed by ring backbones can greatly affect the LC phase transitions and photoinduced anisotropy of whole macromolecules. Being a fascinating class of macromolecules from both structural and functional perspectives, cyclic SCLCPs might be able to provide a versatile platform to engineer various soft nanomaterials, particularly in the areas of biotechnology and advanced healthcare materials.[9b-9d] Therefore, it is very interesting to develop efficient strategies

[a] Jiangsu Key Laboratory of Advanced Functional Polymer Design and Application, College of Chemistry, Chemical Engineering and Materials Science, Soochow University, Suzhou, 215123, China. E-mail: xlzhu@suda.edu.cn, nczhou@suda.edu.cn, xfchen75@suda.edu.cn
[b] Department of Chemistry and Biochemistry, University of California, San Diego, 9500 Gilman Dr., La Jolla, CA 92093, USA.
† Electronic Supplementary Information (ESI) available. See
DOI: 10.1039/x0xx00000x

for rapid construction of new kinds of cyclic SCLCPs with high biocompatibility and superior bioactivity. Furthermore, the systematical investigations on their structure-property relationships are also highly desirable.

In nature, cholesterol is heterogeneously distributed in cellular membranes, and with the roles of modulating the physicochemical properties of the whole membrane.[10] It plays an important role in membrane trafficking, sorting processes, and cell signalling processes.[10] More interestingly, most of cholesterol esters and its derivatives could exhibit LC behaviors since cholesterol consists of a rigid planar subunit and a flexible side chain 'tail'.[10,11a] In the recent years, the cholesterol-modified SCLCPs have been well documented for color information technology, optoelectronics, bioactive-materials and biotechnology.[11] Thus, we believe that the macrocyclic SCLCPs tethered with cholesteryl mesogens at the side chains can be regarded as an interesting class of biological topological SCLCPs with various potential applications.

In this work, for the first time, we synthesize series of novel biomacrocyclic cholesteryl-containing SCLCPs with three different length methylene spacers (m = 2, 6, 11) *via* the combination of reversible addition-fragmentation chain transfer (RAFT) polymerization with Cu(I)-catalyzed azide–alkyne cycloaddition (CuAAC) "click" reaction. Herein, we are very interested in two issues via the elaboration of the model polymers: (1) to develop high-efficiency strategies for preparing new-style cyclic polymers containing various functional groups; (2) to systematically study the liquid crystalline (LC) phase behaviors of cyclic SCLCPs for facilitating the general understanding of their structure-property.

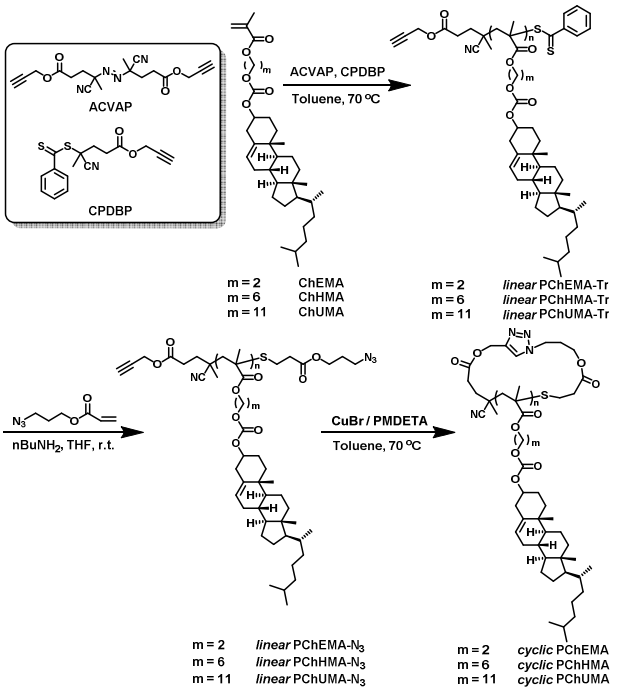

Scheme 1 The synthetic routes towards linear and cyclic cholesteryl-containing SCLCPs.

Experimental

Materials

Cholesteryl chloroformate (Alfa Aesar, 98%), potassium methacrylate (HWRK Chem. , China, 98%), hydroxyethyl methacrylate (HEMA, TCI), sodium azide (NaN_3, Sigma-Aldrich, ≥ 99.5%), 3-bromo-1-propanol, acryloyl chloride, 6-bromo-1-hexanol, 11-bromo-1-undecanol, tetraoctylammonium bromide, Propargyl alcohol were purchased from Energy Chemical and used as received. Azobis (4-cyano valeric acid) (ACVA), dicyclohexylcarbodiimide (DCC), 4-dimethylaminopyridine (DMAP), *N,N,N′,N″,N″*-pentamethyldiethylenetriamine (PMDETA) were purchased from J&K Scientific Ltd. and used as received. Copper(I) bromide (CuBr, Adamas) was freshly purified by stirring in acetic acid overnight, washed with acetone, and dried in vacuum. Triethylamine, pyridine, tetrahydrofuran (THF), acetone, benzene, dichloromethane and all other chemicals were purchased from Sinopharm Chemical Reagent Co., Ltd. without any further purification. 6-hydroxyhexyl methacrylate and 11-hydroxylundecyl methacrylate were synthesized by heating potassium methacrylate with 6-bromo-1-hexanol or 11-bromo-1-undecanol in THF and tetraoctylammonium bromide as a phase transfer catalyst, respectively.[11g,12a] 4-Cyanopentanoic acid dithiobenzoate was synthesized as reported.[12b]

Characterization

The number-average molecular weight (M_n) and polydispersity (M_w/M_n) of the polymers were determined by a TOSOH HLC-8320 size exclusion chromatography equipped with refractive-index and UV detectors using two TSKgel Super Mutipore HZ-N (4.6×150 mm, 3 μm beads size) columns arranged in series, and it can separate polymers in the molecular weight range from 500~1.9×10^5 g/mol. THF was used as the eluent at a flow rate of 0.35 mL/min at 40 °C. Data acquisition was performed using EcoSEC software, and molecular weights were calculated with polymethyl methacrylate (PMMA) standards. Detection of TD-SEC consisted of a RI detector (Optilab rEX), a multi-angle (14-145°) laser light scattering detector (DAWN HELEOS) with the He-Ne light wave length at 658.0 nm, and online viscosity detector (viscoSTAR). THF was used as the eluent at a flow rate of 1.0 mL/min at 35 °C. Three detectors were calibrated with PS standard. The refractive index increment (dn/dc) values were measured offline by using an Optilab rEX refractive index detector (λ = 658 nm), which were conducted in THF at 25 °C with a flow rate of 0.5 mL/min. FT-IR spectra were obtained on a Bruker TENSOR-27 FT-IR spectrometer by mixing polymer with KBr as tablets. ^{1}H NMR spectra were collected using a Bruker nuclear magnetic resonance instrument (300 MHz) using tetramethylsilane (TMS) as the internal standard at room temperature, NMR samples were prepared with concentration of ~20 mg/mL in $CDCl_3$. Thermal behavior and phase transition of all the polymers were observed and obtained using a 2010 DSC V4.4E instrument, which was calibrated by pure indium for temperature and enthalpy changes. Samples with a typical mass about 4 mg were encapsulated in sealed aluminum pans. The DSC heating and cooling traces were recorded with a rate

of 10 °C/min under a continuous N_2 flow. LC textures and birefringence of samples were examined under a POM (Olympus Corporation, BX51-P) equipped with a hot stage (Linkam THMS600). Samples were prepared by sandwiching the polymer powder between a glass slide and a cover glass. Typical LC textures could be formed when heating the sample to its isotropic temperature and then cooling to LC state at a rate of 0.5-1 °C/min. SAXS experiments were used to identify the phase structures of the LCs, which were performed using a high-flux X-ray instrument (SAXSess mc^2, Anton Paar) equipped with line collimation system and a 2200 W sealed-tube X-ray generator (CuKα, λ = 0.154 nm). Samples were wrapped into aluminum foils and sandwiched in a steel sample holder. The X-ray scattering patterns were recorded in vacuum on an imaging-plate (IP). The scattering peak positions were calibrated with silver behenate. A temperature control unit (Anton paar TC300) in conjunction with the SAXSess mc^2 was utilized to study the structure evolution as a function of temperature.

Synthetic procedures

Synthesis of terminal alkyne modified-dithiobenzoate agent (CPDBP): Propargyl alcohol (0.56 g, 10.0 mmol), N,N'-dicyclohexyl carbide imine (DCC, 2.10 g, 10.0 mmol) and dimethylaminopyridine (DMAP, 0.12 g) were dissolved in dry CH_2Cl_2 (50 mL), the solution was stirred and cooled to 0 °C, then a solution of 4-cyanopentanoic acid dithiobenzoate (2.80 g, 10.0 mmol) in dry CH_2Cl_2 (10 mL) was added dropwise. The mixture was stirred at 0 °C for additional 30 min and then at ambient temperature overnight. The salts were removed by filtration and volatiles were removed under reduced pressure, the crude product was purified by column chromatography (ethyl acetate/hexane = 1/10) to yield the red oil (2.3 g). Yield: 72%. ^{1}H NMR ($CDCl_3$, 300 MHz, ppm): 1.94 (s, 3H, C(CH_3)(CN)), 2.49 (d, 1H, C≡CH), 2.5-2.8 (m, 4H, -CH_2-CH_2), 4.72 (d, 2H, OCH_2), 7.30-7.95 (m, 5H, C_6H_5).

Synthesis of terminal alkyne modified initiator (ACVAP): Propargyl alcohol (2.0 g, 35.7 mmol), DCC (9.2 g, 44.6 mmol) and DMAP (0.43 g) were dissolved in dry THF (100 mL), the solution was stirred and cooled to 0 °C and then a solution of ACVA (5.0 g, 17.8 mmol) in dry THF (20 mL) was added dropwise. The mixture was stirred at 0 °C for additional 30 min and then at ambient temperature overnight. The salts were removed by filtration and volatiles were removed under reduced pressure, the crude product was purified by column chromatography (ethyl acetate/hexane = 1/4) to yield the white solid (2.4 g). Yield: 38%. ^{1}H NMR ($CDCl_3$, 300 MHz, ppm): 4.72 (4H, t, CH_2-O-), 2.5 (10H, m, HC≡C-CH_2, COCH_2CH_2C), 1.74 (6H, d, CCH_3).

Synthesis of linear PChHMA-Tr: In a representative procedure, ChHMA (2.0 g, 3.42 mmol), CPDBP (16.4 mg, 0.11 mmol), ACVAP (23.4 mg, 0.11 mmol), and toluene (4.0 mL) were charged into a 10 mL flask and degassed by three freeze-pump-thaw cycles. The flask was then filled with Ar and placed in an oil bath thermostated at 70 °C. After a predetermined time, the flask was cooled and exposed to air and diluted with THF and the polymer was precipitated in a large amount of methanol. The precipitation procedure was repeated three times, after drying in a vacuum oven overnight at 25 °C, the red polymer linear PChHMA-Tr was obtained (1.40 g, yield: 70%).

Synthesis of linear PChHMA-N_3: The polymer was synthesized by a one-pot aminolysis/Michael-addition sequential end group transformation. A 25 mL round-bottom flask was charged with linear PChHMA-Tr (1.0 g, 0.07 mmol) and THF (12 mL). After complete dissolution of the polymer, the solution was degassed by bubbling Ar for at least 40 min, then 3-azidopropyl acrylate (253.2 mg, 1.63 mmol) and n-butylamine (119.2 mg, 1.63 mmol) were added to the solution. The mixture was allowed to stir at room temperature for 5 h under Ar atmosphere. The polymer was recovered by precipitation into an excess of methanol, after filtered and dried in a vacuum oven overnight at 25 °C, the white polymer linear PChHMA-N_3 was obtained (0.94 g, yield: 94%).

Synthesis of cyclic PChHMA: Toluene (700 mL) was added into a 1 L three-necked round-bottom flask and bubbled with Ar for 4 h to remove oxygen. Then CuBr (203.0 mg, 1.42 mmol) and PMDETA (368.0 mg, 2.12 mmol) were charged into the flask under protection of Ar flow. The degassed linear precursor (0.10 g, 0.007 mmol) in 20 mL of toluene was added into the CuBr/PMDETA mixture at 70 °C *via* syringe pump very slowly, over 40 h. After the addition of polymer solution was completed, the reaction was allowed to proceed for another period of 24 h. Then, azide resin (100 mg) was added, after 12 h, the mixture was cooled to room temperature and passed through a silica gel column to remove the metal salt. After most of the solvents were removed by a rotary evaporator, the residue was precipitated into methanol. After drying in a vacuum oven overnight at 30 °C, cyclic PChHMA was obtained (0.074 g, yield: 74%).

Results and discussion

Synthesis and characterization of linear and cyclic cholesteryl-containing SCLCPs

Three methacrylate-derived monomers bearing a pendent cholesteryl group with different methylene spacers were designed and synthesized *via* the esterification reaction between cholesteryl chloroformate and 2-hydroxyethyl methacrylate, 6-hydroxyhexyl methacrylate, or 11-hydroxylundecyl methacrylate, respectively (as shown in Scheme S1).[11g,12a] The molecular structures of related products (ChEMA, ChHMA and ChUMA) can be confirmed by ^{1}H NMR spectra shown in Figure S1-S3. In general, macrocyclic precursors with highly reactive functionality at both chain-end positions are the prerequisites towards macrocyclic polymers using "click" cyclization strategy. In this work, our initial attempts to prepare α-alkyne-ω-azide polymeric linear precursors by atom transfer radical polymerization (ATRP) using an alkyne-bearing initiator were largely unsuccessful, since the terminal bromide of the resulting cholesteryl-functionalized polymethacrylates is very difficult for a complete nucleophilic displacement with an azide (related synthetic route is shown in Scheme S4). It may be accountable

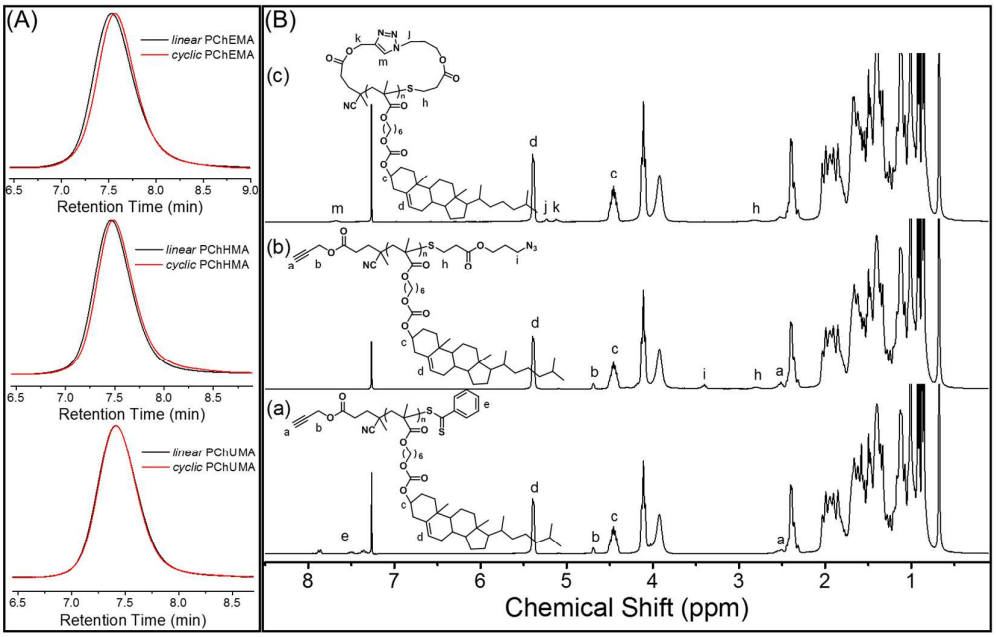

Fig. 1 SEC traces (A) of *linear* PChEMA and *cyclic* PChEMA, *linear* PChHMA and *cyclic* PChHMA, *linear* PChUMA and *cyclic* PChUMA; ^{1}H NMR spectra (B) of (a) *linear* PChHMA-Tr, (b) *linear* PChHMA-N_3, and (c) *cyclic* PChHMA.

that steric hindrance of both bulky hydrophobic cholesterol group and the terminal tertiary-carbon bromine depress the substitution reaction.[13] Alternatively, RAFT polymerization is known as another kind of convenient controlled/living free radical polymerization.[14] Particularly, RAFT polymerization can be conducted under less stringent conditions and offers predominant versatility in terms of monomer choice. Furthermore, the thiocarbonylthio end group of the resultant RAFT polymer can be easily converted into a "clickable" thiol group *via* aminolysis, followed by modification with functional group *via* thiol-based "click" chemistry.[15] According to the mechanism of RAFT polymerization, the polymers obtained by RAFT inevitably contain some initiator moieties at the *α*-chain-end.[16] Therefore, we used the initiator that has the same alkynyl structure as R group in RAFT agent to improve the degree of chain end functionality in high yields (as shown in scheme 1). Consequently, we prepared the linear polymers with three length methylene spacers (m = 2, 6, 11) by performing the RAFT polymerization in the presence of a terminal alkyne modified chain transfer agent CPDBP. The polymers with similar degrees of polymerization (n) ranged from 21 to 24 were obtained by controlling the molar ratio of monomer to CPDBP and polymerization conversion, which were supported by end-group analysis of the ^{1}H NMR spectra. The azidation modification of terminal dithiobenzoate groups of RAFT polymer was carried out *via* aminolysis/Michael addition sequence in THF at room temperature in a one-pot fashion. As expected, *α*-alkyne-*ω*-azide linear precursors were efficiently obtained, as shown in Scheme 1. From ^{1}H NMR spectra in Figure 1(B), Figure S4 and Figure S7, the emergence of a resonance peak at 3.40 ppm after aminolysis/Michael addition, corresponded to the methylene protons adjacent to the terminal azide group, and the disappearance of dithiobenzoate protons of RAFT polymers at 7.35, 7.50 and 7.80 ppm, could confirm that the chemical transformation of the end groups was completed. The SEC elution traces of azido-end polymers are in good agreement with that of RAFT polymers respectively, due to the slightly difference in molecular weight. Further evidence for the azide-end polymers could be observed in FT-IR spectra, by monitoring the appearance of the azide group at ~2100 cm^{-1} (Figure S5, Figure S6 and Figure S8).

The concentration of the staring linear polymer precursors in solution is a critical factor during the cyclization procedure.[13] This cyclization reaction was performed at the high dilute condition (0.14 mg/mL). Meanwhile, a very slow continuous addition of the macrocyclic precursors into toluene solution containing CuBr and PMDETA using a syringe pump was also utilized to maintain the infinitesimal concentration of linear precursors during intramolecular cyclization. The intrachain click reaction of the *α*-alkyne-*ω*-azide macrocyclic precursors gives rise to the desirable cyclic products. The azide resin was used to remove all the uncyclic polymers with alkynyl chain ends. The successful cyclization was confirmed by comprehensive characterization including SEC, TD-SEC, FT-IR and ^{1}H NMR spectra. For example, the SEC curves of cyclic polymers and their corresponding linear counterparts are presented in Figure 1(A). The presence of intermolecular condensation impurities, such as linear dimers is not observed in SEC curves. Cyclic PChEMA and PChHMA display a discernible longer elution time due to decreased hydrodynamic volume compared to their linear counterparts.[1b] In PChUMA case with longer methylene spacers, little difference between cyclic and linear polymers is observed in

Table 1. Characterization of linear and cyclic cholesteryl-containing SCLCPs.

Sample	n[a]	M_n[a] g/mol	M_n[b] g/mol	M_w/M_n[b]	M_n[c] g/mol	M_w[c] g/mol	M_n/M_n[c]	[η][c] mL/g	dn/dc[d] mL/g	T_g °C	T_1 °C	ΔH_1 J·g^{-1}	ΔS_1 J·g^{-1}K^{-1}	T_{cl} °C	ΔH_{cl} J·g^{-1}	ΔS_{cl} J·g^{-1}K^{-1}
linear PChEMA	24	13400	13200	1.12	15700	16200	1.03	6.8	0.116	111.2	-	-	-	206.4	3.21	6.69×10^{-3}
cyclic PChEMA			12800	1.12	16500	16900	1.02	6.5	0.114	113.6	-	-	-	203.1	3.04	6.38×10^{-3}
linear PChHMA	23	14100	14900	1.11	14900	15500	1.04	7.1	0.113	51.9	-	-	-	166.1	4.94	1.12×10^{-2}
cyclic PChHMA			14600	1.11	16000	16300	1.02	6.7	0.112	50.6	-	-	-	162.2	4.65	1.07×10^{-2}
linear PChUMA	21	14400	16600	1.06	15200	16500	1.08	10.1	0.112	42.1	81.9	2.48	6.98×10^{-3}	127.5	1.47	3.67×10^{-3}
cyclic PChUMA			16400	1.07	15800	16600	1.05	8.6	0.113	35.1	77.0	1.48	4.23×10^{-3}	125.6	1.37	3.44×10^{-3}

[a] Determined by ^{1}H NMR spectra. [b] Determined by SEC measurements. [c] Determined by TD-SEC measurements. [d] determined by Wyatt Optilab rEX at five different concentrations.

SEC elution time, possibly because longer side chain leads to a nearly the same hydrodynamic volume for current cyclic and linear polymers.[3c] Moreover, the cyclic architectures were also verified by TD-SEC, and their characterizations are fully summarized in Table 1. The dn/dc values for linear and cyclic polymers were experimentally determined by Wyatt Optilab rEX using five different concentrations, showing the dn/dc values of cyclic polymers are similar to those of linear counterparts, which is consistent with the previous reports.[17] The calculated absolute molecular weights of cyclic polymers are in good agreement with those of linear precursors. Due to the cyclic topology, the [η] values of the cyclic polymers are lower than those of linear counterparts.[17c] As FT-IR spectra shown in Figure S5, Figure S6 and Figure S8, after ring closure, the disappearance of the characteristic azide signals at ~2100 cm^{-1} and alkynyl at ~3300 cm^{-1} provide further evidence for the successful cyclization. The ^{1}H NMR spectra of all linear and cyclic polymers are show in Figure 1(B), Figure S4 and Figure S7, respectively. After the ring closure reaction, the signal of the terminal alkynyl protons at 2.50 ppm in the linear polymer disappears, while a new characteristic signal at 7.68 ppm assigned to the proton of triazole ring is observed. Furthermore, the signals of methylene protons adjacent to the alkyne and the azide groups at 4.70 and 3.40 ppm in the linear polymer shift to 5.23 and 5.10 ppm, respectively, due to the formation of 1,2,3-triazole ring. These results suggest the intramolecular cyclization was successful under high dilution.

Phase transitions and phase structures of linear and cyclic cholesteryl-containing SCLCPs

The phase behaviors of linear and cyclic SCLCPs were first studied by a combination of DSC and POM. Figure 2(A) shows the first cooling and the second heating DSC curves of all samples at a rate of 10 °C/min under N_2 atmosphere after eliminating the thermal history. For cyclic PChEMA and PChHMA, one glass transition and one phase transition peaks could be detected whether in heating or cooling curves. Observation with POM showed that the birefringence disappeared above the phase transition temperatures, indicating they are refer to the isotropic temperatures.[18] Interestingly, two phase transition peaks could be found in both cyclic and linear PChUMA, indicating more complex phase behaviors. Furthermore, POM results indicated the second transition belongs to the isotropic state transition, but a change in the texture was not observed at the first transition, and the further discussion will be shown in the following section of mesomorphic structural analyses. As indicated in Table 1, as the spacer length of methylene increased, glass transition temperature (T_g) decreased for cyclic SCLCPs due to internal plasticization arising from reduced packing density of mesogens.[19] Similarly, clearing temperature (T_{cl}) significantly decreased and sharpened with the increase in spacer length of methylene, which is due to the decoupling the motion between the backbone and cholesteryl mesogens more efficiently.[20] While comparing to the linear polymers, the phase transitions for all the cyclic polymers appear at lower temperatures and with broadened transition endothermic or exothermic peaks due to the topological constraint effect.[9a] The corresponding enthalpies (ΔH_{si}) and entropies (ΔS_{si}) can be calculated according to $\Delta S_{si} = \Delta H_{si}/\Delta T_{si}$, which are also summarized in Table 1. In addition to the slightly lowering of phase temperatures in cyclic polymers, both enthalpies and entropies are smaller than those of linear ones, which may arise from the topological constraint effect imposed by the cyclic architectures.[9a] Generally, the smaller phase transition enthalpies usually indicate a decreased molecular order of mesogens in the LC phases of cyclic polymers and reduced intermolecular interactions.[9a,21] As for the smaller phase transition entropies suggest a reduction of polymer chain mobility in the isotropic phase with respect to the LC phase.[9a]

Despite the presence of eight chiral centers in cholesterol, polymethacrylates comprising cholesteryl side-chains are in favor to form smectic mesophases.[18,22] The most striking difference for the chemical structure of the linear SCLCPs in this article is to change the ester bond to a carbonate linkage, which connect the cholesteryl mesogen and flexible spacer together. Figure 2(B) shows the POM images of the linear and cyclic SCLCPs, which were taken in the course of cooling from the isotropic phase respectively. The typical focal conic texture could be observed for the linear and cyclic polymers, indicating the formation of the smectic phase.[18] It could be found that

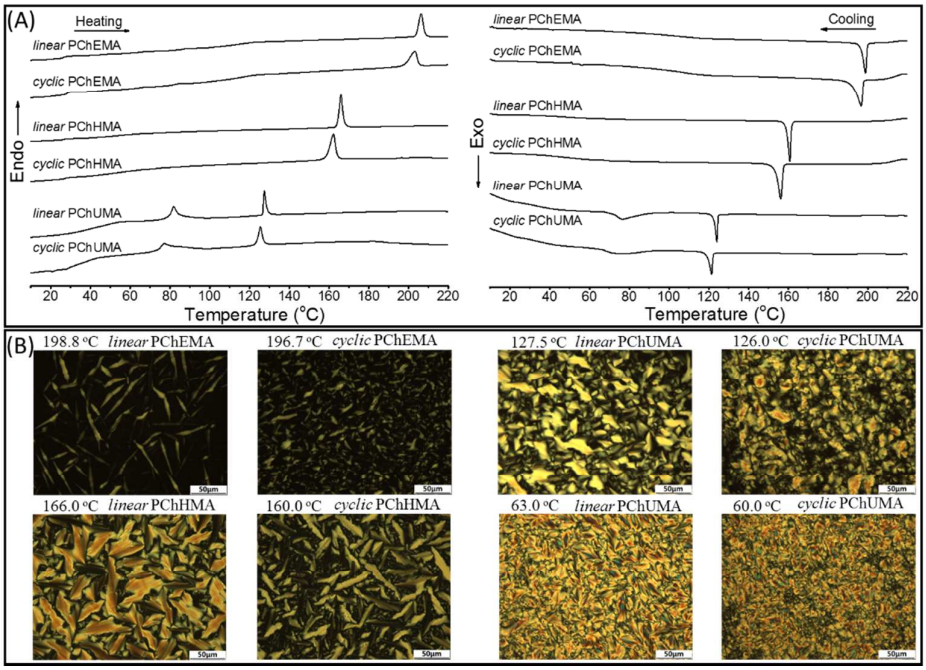

Fig. 2 DSC heating and cooling curves (A) of linear and cyclic cholesterol-containing SCLCPs (second scan); Polarizing optical micrographs (B) of *linear*, *cyclic* PChEMA, *linear*, *cyclic* PChHMA, and *linear*, *cyclic* PChUMA, recorded upon cooling from isotropic phase, respectively.

the cyclic polymer samples exhibit smaller textures than those of linear polymer samples under POM. This result may arise from the topological constraint effect that causes more defects in the cyclic SCLCPs, which is similar to that in cyclic azobenzene-containing SCLCPs.[9a]

To further study the phase transitions and phase structures of the linear and cyclic SCLCPs, SAXS experiments were then performed. Prior to the SAXS experiments, the samples were subjected to a predetermined time of annealing at a certain temperature among liquid crystalline region and then very slowly cooled down to the room temperature. Meantime, to elucidate the packing of mesogens in the mesophase, the experimental interlayer distance was compared to the lamellar spacing *l* calculated using molecular modeling software from ACDlabs FreeView.[22b] *l* is the distance between a carbon atom of the end-methyl group in the cholesterol mesogen (full extended) and the carbon atom of the polymer main chain. Figure 3(A) and 3(B) shows the temperature-dependent SAXS profiles of linear, cyclic PChEMA and linear, cyclic PChHMA, respectively. Below the isotropic temperature, three scattering peaks (although the third one is very week but still noticeable) at low angle region could be observed clearly in cyclic PChEMA with the *q* ratio of 1:2:3, indicating a typical layer-like structure formed. The calculated *d*-spacing from the first scattering vector is 4.60 nm, which is shorter than twice the calculated extended length of the side chain (*l* = 2.50 nm) of cyclic PChEMA. Thus a partially interdigitated smectic A (SmA_d) phase is proposed, as illustrated in Figure 4(a). The linear PChEMA exhibits the SmA_d structure as well with the same layer periodicity as that of the cyclic one, indicating the different topology of polymer backbone doesn't influence much of the mesophase structure parameters. Notably, the layer periodicity decreases gradually as the temperature increases, which can be attributed to the gradual order alignment of the spacers between the main chains and the rigid cholesteryl groups.[22c] The diffraction pattern for both cyclic and linear PChHMA are constituted by three diffraction peaks with the *q* ratio of 1:2:3, suggesting the presence of a long-range-ordered lamellar structure with a period of 5.35 nm. The layer periodicity is between *l* and 2*l* (*l* = 3.01 nm, the calculated extended length of the side chain), which indicates that PChHMA also shows a SmA_d phase, as illustrated in Figure 4(b). It is worth noting that with increasing the length of methylene spacer, diffraction peaks became more distinct and sharper, which can be attributed to the enhanced mesogen orientation by the decoupling effect of longer flexible methylene spacer between main chain and mesogenic side chain.[18,20,23] This result correlates well with the high enthalpy value of T_{cl} in PChHMA observed by DSC. Therefore, although the cyclic topology does not have a significant effect on the formation of smectic structure, it still imposes an influence on mesophase transition temperature, enthalpy and entropy, as described above.

Figure 3(C) shows the temperature dependent SAXS profiles of linear and cyclic PChUMA, respectively. Below the first phase transition temperature, several scattering peaks in the small angle region were observed. The corresponding *d*-spacings of cyclic PChUMA are 6.44, 3.60, and 2.32 nm, respectively, which do not correlate with each other. The *d*-spacing of the first reflection is somewhat less than twice the calculated length of the side chain. Subsequently, two-dimensional X ray scattering patterns of linear and cyclic

PChUMA were thus obtained by shearing the samples within the LC temperature (Figure S9). The first reflection splits into four arcs, probably due to the side chain tilted against the main chain, indicating the existence of typical smectic C (SmC) structure.[5b,24a] Differed from first one, the second reflection splits into two arcs. The corresponding *d*-spacing is 3.60 nm of the second reflection, which is close to the calculated length of the side chain of 3.66 nm, indicating a monolayer smectic A (SmA_1) structure could also be found in this phase. The third reflection can be attributed to the sub-plane composed of cholesterol mesogens and the overlapping alkyl chains. The coexistence of two different types of smectic layers has been rationalized for spacer lengths of 9-11 methylene groups in polymethacrylates or 9-10 methylene groups in polynorbornenes containing cholesteryl side-chains.[18,22b,24] So we speculate that PChUMA initially includes the packing structures of both SmC and SmA_1 layers at low temperature, as illustrated in Figure 4(c). When further increasing temperature above the first transition temperature around 80 °C, the first and the third scattering peaks in SAXS patterns disappear and the SmC structure enters isotropic, while the second scattering peak remains there with decreased intensity, implying that the SmA_1 layer structure coexists with the isotropic phase in the temperature region between the two transitions.[18,24c,24d]

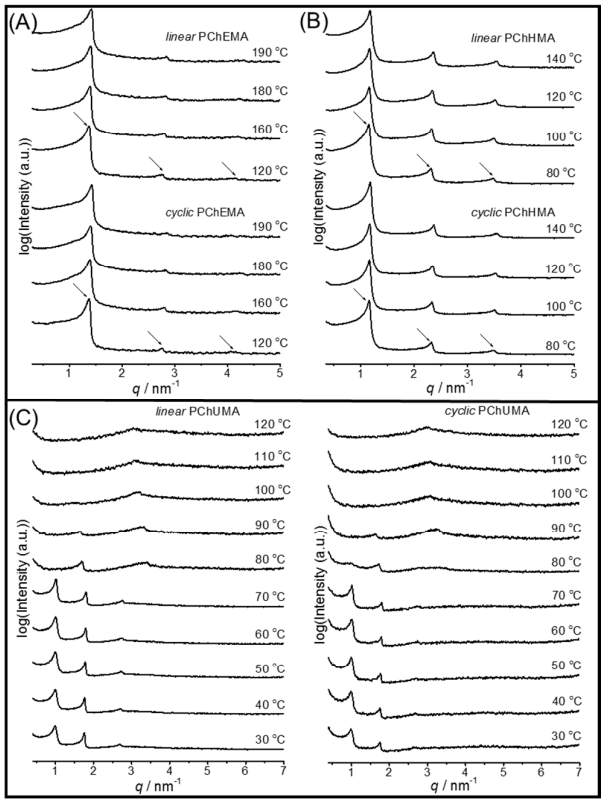

Fig. 3 SAXS profiles of (A) *linear*, *cyclic* PChEMA, (B) *linear*, *cyclic* PChHMA, and (C) *linear*, *cyclic* PChUMA recorded, respectively.

Notably, a new reflection appears at the same time, corresponding to a *d*-spacing of 1.84 nm, and the ratio of their reciprocal spacing is 1:2. Significantly, when further increasing the temperature, the second scattering peak decreases progressively in intensity and finally vanishes at 100 °C, before the transition to the isotropic phase. In contrast, the new reflection corresponding to a *d*-spacing of 1.84 nm remains throughout this mesophase.

Furthermore, the relative proportions of the two phases can be qualitatively estimated from the intensities of the associated reflections in Figure 3(C). For linear PChUMA, the intensity of second peak is weaker than that of the first peak. After cyclization, the intensity of the three reflections sharply decreased in turn, implying the cyclic polymer has a greater proportion of SmC mesophase structure than the linear one.[18,24c,24d] This may because that the restriction of cyclic topology in main chain coupled with steric hindrance of bulky cholesterol mesogens in the side chain weaken the mobility of the side chain ends in the monolayer packing structure.[18,24c,24d] As a result, the formation of fully interdigitated packing mode is somewhat hindered in cyclic polymer, leading to its LC mesogens order form SmC phase more easily than SmA_1 phase.

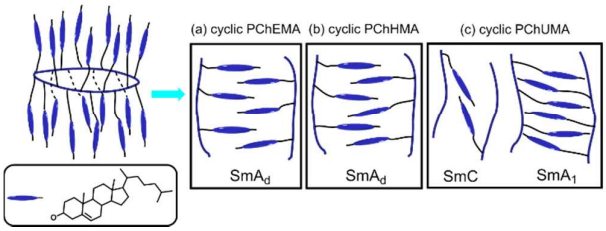

Fig. 4 Schematic illustrations of the packing structures of cyclic cholesteryl-containing SCLCPs with different length methylene spacer: (a) partial overlapped bilayer packing structure in cyclic PChEMA; (b) partial overlapped bilayer packing structure in cyclic PChHMA; (c) coexistence of partial bilayer SmC packing structure (left) and monolayer packing structure (right) in cyclic PChUMA.

Conclusions

In summary, biomacrocyclic cholesterol-containing side-chain liquid crystalline polymers with three different lengths of methylene spacers are successfully prepared for the first time *via* the combination of RAFT polymerization with CuAAC "click" reaction. The formation of cyclic SCLCPs is fully characterized and verified by SEC, TD-SEC, FT-IR and ^{1}H NMR spectra. The described cyclization strategy is expected to be particularly useful for preparing a variety of well-defined cyclic polymers containing bulky hydrophobic groups, owing to the excellent monomer choice in a wide range and molecular weight control of RAFT polymerization. On the basis of the POM, DSC and SAXS results, both linear and cyclic SCLCPs form the smectic phase among the LC region with the same layer periodicity. Moreover, cyclic polymers exhibit a slightly lower mesophase transition temperature, enthalpy, entropy and smaller textures microstructures than the linear counterparts. Interestingly, the SmC packing structure is preferable in cyclic PChUMA compared with that in the linear one. Overall, this study not only provides better understanding for structure-property

relationship in SCLCPs, but also facilitates the development of programmable materials with various potential applications such as optoelectronics and bioactive materials. Further investigations on the construction of those biomacrocycle-based smart nano-materials as drug carriers and biosensors for specific diagnostic and therapeutic purposes are currently in progress in our research group.

Acknowledgements

This work was supported by the National Science Foundation of China (21234005, 21474068), the Priority Academic Program Development of Jiangsu Higher Education Institutions (PAPD) and the Program of Innovative Research Team of Soochow University.

Notes and references

1 (a) K. Endo, *New Frontiers in Polymer Synthesis*, 2008, **217**, 121; (b) B. A. Laurent and S. M. Grayson, *Chem. Soc. Rev.*, 2009, **38**, 2202; (c) H. R. Kricheldorf, *J. Polym. Sci., Part A: Polym. Chem.*, 2010, **48**, 251; (d) T. Yamamoto and Y. Tezuka, *Polym. Chem.* 2011, **2**, 1930; (e) Z. Jia and M. J. Monteiro, *J. Polym. Sci., Part A: Polym. Chem.*, 2012, **50**, 2085; (f) R. J. Williams, A. P. Dove and R. K. O'Reilly, *Polym. Chem.*, 2015, **6**, 2998.

2 (a) S. Honda, T. Yamamoto and Y. Tezuka, *J. Am. Chem. Soc.*, 2010, **132**, 10251; (b) M. D. Hossain, D. Lu, Z. Jia and M. J. Monteiro, *ACS Macro Lett.*, 2014, **3**, 1254; (c) X. Zhu, N. Zhou, Z. Zhang, B. Sun, Y. Yang, J. Zhu and X. Zhu, *Angew. Chem., Int. Ed.*, 2011, **50**, 6615; (d) J. E. Poelma, K. Ono, D. Miyajima, T. Aida, K. Satoh and C. J. Hawker, *ACS Nano*, 2012, **6**, 10845; (e) K. Zhang, M. A. Lackey, J. Cui and G. N. Tew, *J. Am. Chem. Soc.*, 2011, **133**, 4140; (f) R. A. Perez, J. V. Lopez, J. N. Hoskins, B. Zhang, S. M. Grayson, M. T. Casas, J. Puiggali and A. J. Muller, *Macromolecules*, 2014, **47**, 3553; (g) T. S. Stukenbroeker, D. Solis-Ibarra and R. M. Waymouth, *Macromolecules*, 2014, **47**, 8224; (h) D. Magerl, M. Philipp, X. P. Qiu, F. M. Winnik and P. Müller-Buschbaum, *Macromolecules*, 2015, **48**, 3104.

3 (a) B. Chen, K. Jerger, J. M. J. Frechet and F. C. Szoka, *J. Controlled Release*, 2009, **140**, 203; (b) X. Wan, T. Liu and S. Liu, *Biomacromolecules*, 2011, **12**, 1146; (c) H. Wei, D. S. H. Chu, J. Zhao, J. A. Pahang and S. H. Pun, *ACS Macro Lett.*, 2013, **2**, 1047; (d) M. A. Cortez, W. T. Godbey, Y. Fang, M. E. Payne, B. J. Cafferty, K. A. Kosakowska and S. M. Grayson, *J. Am. Chem. Soc.*, 2015, **137**, 6541.

4 (a) J. Lu, A. Xia, N. Zhou, W. Zhang, Z. Zhang, X. Pan, Y. Yang, Y. Wang and X. Zhu, *Chem. Eur. J.*, 2015, **21**, 2324; (b) B. Chen, Z. Wang, J. Lu, X. Yang, Y. Wang, Z. Zhang, J. Zhu, N. Zhou, Y. Li and X. Zhu, *Polym. Chem.*, 2015, **6**, 3009; (c) Y. Sun, Z. Wang, Y. Li, Z. Zhang, W. Zhang, X. Pan, N. Zhou and X. Zhu, *Macromol. Rapid Commun.*, 2015, **36**, 1341.

5 (a) J. J. Ge, S. C. Hong, B. Y. Tang, C. Y. Li, D. Zhang, F. Bai, B. Mansdorf, F. W. Harris, D. Yang, Y. R. Shen and S. Z. D. Cheng, *Adv. Funct. Mater.*, 2003, **13**, 718; (b) J. F. Zheng, X. Liu, X. Chen, X. K. Ren, S. Yang and E. Q. Chen, *ACS Macro Lett.*, 2012, **1**, 641; (c) Z. Q. Yu, T. T. Li, Z. Zhang, J. H. Liu, W. Z. Yuan, J. W. Y. Lam, S. Yang, E. Q. Chen and B. Z. Tang, *Macromolecules*, 2015, **48**, 2886; (d) X. F. Chen, Z. Shen, X. H. Wan, X. H. Fan, E. Q. Chen, Y. Ma and Q. F. Zhou, *Chem. Soc. Rev.*, 2010, **39**, 3072; (e) K. Ichimura, *Chem. Rev.*, 2000, **100**, 1847; (f) M. Yamada, M. Kondo, J. I. Mamiya, Y. Yu, M. Kinoshita, C. J. Barrett and T. Ikeda, *Angew. Chem., Int. Ed.*, 2008, **47**, 4986.

6 (a) E. R. Zubarev, R. V. Talroze, T. I. Yuranova, N. A. Plate and H. Finkelmann, *Macromolecules*, 1998, **31**, 3566; (b) J. Barbera, B. Donnio, L. Gehringer, D. Guillon, M. Marcos, A. Omenat and J. L. Serrano, *J. Mater. Chem.*, 2005, **15**, 4093; (c) T. Ganicz, T. Pakula, W. Fortuniak and E. Bialecka-Florjanczyk, *Polymer*, 2005, **46**, 11380; (d) N. Canilho, E. Kasemi, A. D. Schluter, J. Ruokolainen and R. Mezzenga, *Macromolecules*, 2007, **40**, 7609; (e) M. Marcos, R. Martin-Rapun, A. Omenat and J. L. Serrano, *Chem. Soc. Rev.*, 2007, **36**, 1889; (f) J. Ping, Y. Qiao, H. Tian, Z. Shen and X. H. Fan, *Macromolecules*, 2015, **48**, 592; (g) L. Han, H. Ma, Y. Li, J. Wu, H. Xu and Y. Wang, *Macromolecules*, 2015, **48**, 925; (h) T. Felekis, L. Tziveleka, D. Tsiourvas and C. M. Paleos, *Macromolecules*, 2005, **38**, 1705; (i) A. M. Kasko, A. M. Heintz and C. Pugh, *Macromolecules*, 1998, **31**, 256.

7 (a) V. Percec, A. D. Asandei and P. Chu, *Macromolecules*, 1996, **29**, 3736; (b) V. Percec, P. J. Turkaly and A. D. Asandei, *Macromolecules*, 1997, **30**, 943.

8 (a) X. Mei, Y. Chu, J. Cui, Z. Shen and X. Wan, *Macromolecules*, 2010, **43**, 8942; (b) X. Mei, J. Zhang, Z. Shen and X. Wan, *Polym. Chem.*, 2012, **3**, 2857.

9 (a) D. Han, X. Tong, Y. Zhao, T. Galstian and Y. Zhao, *Macromolecules*, 2010, **43**, 3664; (b) L. Jia, D. Cui, J. Bignon, A. Di Cicco, J. Wdzieczak-Bakala, J. Liu and M. H. Li, *Biomacromolecules*, 2014, **15**, 2206; (c) C. T. Nguyen, T. H. Tran, X. Lu and R. M. Kasi, *Polym. Chem.*, 2014, **5**, 2774; (d) T. H. Tran, C. T. Nguyen, L. Gonzalez-Fajardo, D. Hargroye, D. Song, P. Deshinukh, L. Mahajan, D. Ndaya, L. Lai, R. M. Kasi and X. Lu, *Biomacromolecules*, 2014, **15**, 4363.

10 L. Hosta-Rigau, Y. Zhang, B. M. Teo, A. Postma and B. Stadler, *Nanoscale*, 2013, **5**, 89.

11 (a) Y. Zhou, V. A. Briand, N. Sharma, S. K. Ahn and R. M. Kasi, *Materials*, 2009, **2**, 636; (b) J. H. Liu and F. M. Hsieh, *Mater. Chem. Phys.*, 2009, **118**, 506; (c) Y. Wang, B. Y. Zhang, X. Z. He and J. W. Wang, *Colloid. Polym. Sci.*, 2007, **285**, 1077; (d) H. Yang, M. X. Liu, Y. W. Yao, P. Y. Tao, B. P. Lin, P. Keller, X. Q. Zhang, Y. Sun and L. X. Guo, *Macromolecules*, 2013, **46**, 3406; (e) Y. S. Freidzon, Y. G. Tropsha, V. P. Shibaev and N. A. Plate, *Makromol. Chem., Rapid Commun.*, 1985, **6**, 625; (f) V. P. Shibaev, N. A. Plate and Y. S. Freidzon, *J. Polym. Sci., Part A: Polym. Chem.*, 1979, **17**, 1655; (g) P. J. Shannon, *Macromolecules*, 1984, **17**, 1873; (h) P. Deshmukh, S. K. Ahn, L. G. de Merxem and R. M. Kasi, *Macromolecules*, 2013, **46**, 8245; (i) P. Deshmukh, S. K. Ahn, M. Gopinadhan, C. O. Osuji and R. M. Kasi, *Macromolecules*, 2013, ***46***, 4558; (j) S. K. Ahn and R. M. Kasi, *Adv. Funct. Mater.*, 2011, **21**, 4543.

12 (a) P. J. Shannon, *Macromolecules*, 1983, **16**, 1677; (b) Y. Mitsukami, M. S. Donovan, A. B. Lowe and C. L. McCormick, *Macromolecules*, 2001, **34**, 2248.

13 B. A. Laurent and S. M. Grayson, *J. Am. Chem. Soc.*, 2006, **128**, 4238.

14 G. Moad, E. Rizzardo and S. H. Thang, *Aust. J. Chem.*, 2012, **65**, 985.

15 (a) X. P. Qiu, F. Tanaka and F. M. Winnik, *Macromolecules*, 2007, **40**, 7069; (b) X. P. Qiu, E. V. Korchagina, J. Rolland and F. M. Winnik, *Polym. Chem.*, 2014, **5**, 3656.

16 Y. Wu, W. Zhang, Z. Zhang, X. Pan, Z. Cheng, J. Zhu and X. Zhu, *Chem. Commun.*, 2014, ***50***, 9722.

17 (a) H. Durmaz, A. Dag, G. Hizal and U. Tunca, *J. Polym. Sci., Part A: Polym. Chem.*, 2010, 48, 5083; (b) H. Durmaz, A. Dag, G. Hizal and U. Tunca, *J. Polym. Sci., Part A: Polym. Chem.*, 2011, **49**, 1195; (c) Y. Cai, J. Lu, F. Zhou, X. Zhou, N. Zhou, Z. Zhang and X. Zhu, *Macromol. Rapid Commun.*, 2014, **35**, 901.

18 T. Yamaguchi, T. Asada, H. Hayashi and N. Nakamura, *Macromolecules*, 1989, **22**, 1141.

19 C. Pugh and A. L. Kiste, *Prog. Polym. Sci.*, 1997, **22**, 601.

20 H. Finkelmann, H. Ringsdorf and J. H. Wendorff, *Macromol. Chem. Phys.*, 1978, **179**, 273.
21 Y. F. Zhu, Z. Y. Zhang, Q. K. Zhang, P. P. Hou, D. Z. Hao, Y. Y. Qiao, Z. Shen, X. H. Fan and Q. F. Zhou, *Macromolecules*, 2014, **47**, 2803.
22 (a) V. S. Freidzon, A. V. Kharitonov, V. P. Shibaev and N. A. Plate, *Eur. Polym. J.*, 1985, **21**, 211; (b) I. W. Hamley, V. Castelletto, P. Parras, Z. B. Lu, C. T. Imrie and T. Itoh, *Soft Matter*, 2005, **1**, 355; (c) Y. Zhu, Y. Zhou, Z. Chen, R. Lin and X. Wang, *Polymer*, 2012, **53**, 3566.
23 S. K. Ahn, L. T. N. Le and R. M. Kasi, *J. Polym. Sci., Part A: Polym. Chem.*, 2009, **47**, 2690.
24 (a) S. K. Ahn, M. Gopinadhan, P. Deshmukh, R. K. Lakhman, C. O. Osuji and R. M. Kasi, *Soft Matter*, 2012, **8**, 3185; (b) G. Galli, E. Chiellini, M. Laus, A. S. Angeloni, O. Francescangeli and B. Yang, *Macromolecules*, 1994, **27**, 303; (c) J. H. Zhang, C. G. Bazuin, S. Freiberg, F. Brisse and X. X. Zhu, *Polymer*, 2005, **46**, 7266; (d) T. Yamaguchi and T. Asada, *Liq. Cryst.*, 1991, **10**, 215.